Supporting Information

Amin et al. 10.1073/pnas.0812469106

SI Materials and Methods

Fly Stocks. *lkb1*$^{4A4-2}$ and *lkb1*$^{4B1-11}$ were induced by ethyl methyl sulfonate (EMS) on the FRT82B chromosome and identified on the basis of their failure to localize GFP–Staufen to the posterior of the oocyte (1). Other stocks used, *lkb1*^{X5} (2), *ampk*α^3 (3), *UAS-MRLC*^{EE} (2), *UAS-RNAi* KP78a (line 47658), KP78b (line 51995), Sik3 (line 39866), and NuAk (line 16334), were obtained from the Vienna *Drosophila* RNAi Center (Vienna, Austria).

Clonal Analysis. Clonal analysis was performed by using the FRT/Flp technique (4) using the following stocks: *eyFLP* or *hsFLP* with *lkb1 FRT 82b/FRT 82b M*$^+$ *UbiGFP* or *hsFLP* with *ampk*α^3 *FRT 101/FRT 101 UbiGFP*. *hsFLP* clones were induced by heat-shocking the larvae for 1 h at 37 °C. Adult mutant eye clones were generated according to the *EGUF/hid* method (5). RNAi lines were crossed to *y w hs FLP122; tub>y+>Gal4 UAS-GFP*. Flip-out clones were induced by heat-shocking 24- to 48-h-old embryos for 40 min at 37 °C.

MARCM Experiments. We used the MARCM technique (6) to examine *lkb1* clones alone or expressing MRLC^{EE} or P35 using: *eyFLP*, *UAS-mCD8::GFP; tubGal80* FRT 82b, *tubGal4*, *UAS-MRLC*^{EE}, or *UAS-P35*, *lkb1 FRT 82b*.

Histochemical Methods. Imaginal discs were fixed and stained by using standard procedures. The primary antibodies used were mouse anti-Arm 1:100 for retinas, 1:400 for discs (DSHB), rabbit anti-PKCζ 1:100 for retinas, and 1:1,000 for discs (Santa Cruz Biotechnology), mouse anti-Crb 1:100 (DSHB), rat anti-Crb 1:100 (E. Knust, Max-Planck Institute MCBG Dresden, Germany and U. Tepass, University of Toronto, Toronto, Canada), rabbit anti-Sdt 1:200 (7), rabbit anti-PatJ 1:2,000 (M. Bhat, University of North Carolina, Chapel Hill, NC), rat anti-Baz 1:500 (A. Wodarz, University of Göttingen, Göttingen, Germany), rabbit anti-Par-6 1:100 (8), rat anti-DE-Cadherin 1:100 (DSHB), rat anti-Bar 1:1,000 (H.M.), mouse anti-Spalt 1:500 (9), mouse anti-Boss 1:1,000 (10). For adult eye anti-Chaoptin immunohistochemistry, *Drosophila* heads were cut in half along the anterior-to-posterior axis and fixed overnight at 4 °C in 4% paraformaldehyde/PBS. Subsequently, the heads were cryoprotected in 20% sucrose/PBS overnight at 4 °C and then embedded in HistoPrep (Fisher Scientific) for frozen horizontal-cut 14-μm cryostat sections. Anti-Chaoptin (mAb24B10; DSHB) was used at a 1:20 dilution with the indirect HRP-method (Vectastain elite; Vector Laboratories). For transmission EM, the heads were fixed with glutaraldehyde/cacodylate and postfixed with osmium tetroxide/cacodylate according to the methods described (11) and cut into 60-nm sections with a diamond knife and then stained with uranyl acetate (4%) and Reynolds' lead citrate for 7 min.

1. Martin SG, St Johnston D (2003) A role for *Drosophila* LKB1 in anterior–posterior axis formation and epithelial polarity. *Nature* 421:379–384.
2. Lee JH, et al. (2007) Energy-dependent regulation of cell structure by AMP-activated protein kinase. *Nature* 447:1017–1020.
3. Mirouse V, Swick LL, Kazgan N, St Johnston D, Brenman JE (2007) LKB1 and AMPK maintain epithelial cell polarity under energetic stress. *J Cell Biol* 177:387–392.
4. Xu T, Rubin GM (1993) Analysis of genetic mosaics in developing and adult *Drosophila* tissues. *Development* 117:1223–1237.
5. Stowers RS, Schwarz TL (1999) A genetic method for generating *Drosophila* eyes composed exclusively of mitotic clones of a single genotype. *Genetics* 152:1631–1639.
6. Lee T, Luo L (2001) Mosaic analysis with a repressible cell marker (MARCM) for *Drosophila* neural development. *Trends Neurosci* 24:251–254.
7. Hong Y, Ackerman L, Jan LY, Jan YN (2003) Distinct roles of Bazooka and Stardust in the specification of *Drosophila* photoreceptor membrane architecture. *Proc Natl Acad Sci USA* 100:12712–12717.
8. Petronczki M, Knoblich JA (2001) DmPAR-6 directs epithelial polarity and asymmetric cell division of neuroblasts in *Drosophila*. *Nat Cell Biol* 3:43–49.
9. Barrio R, de Celis JF, Bolshakov S, Kafatos FC (1999) Identification of regulatory regions driving the expression of the *Drosophila* spalt complex at different developmental stages. *Dev Biol* 215:33–47.
10. Van Vactor DL, Jr, Cagan RL, Kramer H, Zipursky SL (1991) Induction in the developing compound eye of *Drosophila*: Multiple mechanisms restrict R7 induction to a single retinal precursor cell. *Cell* 67:1145–1155.
11. Auld VJ, Fetter RD, Broadie K, Goodman CS (1995) Gliotactin, a novel transmembrane protein on peripheral glia, is required to form the blood-nerve barrier in *Drosophila*. *Cell* 81:757–767.

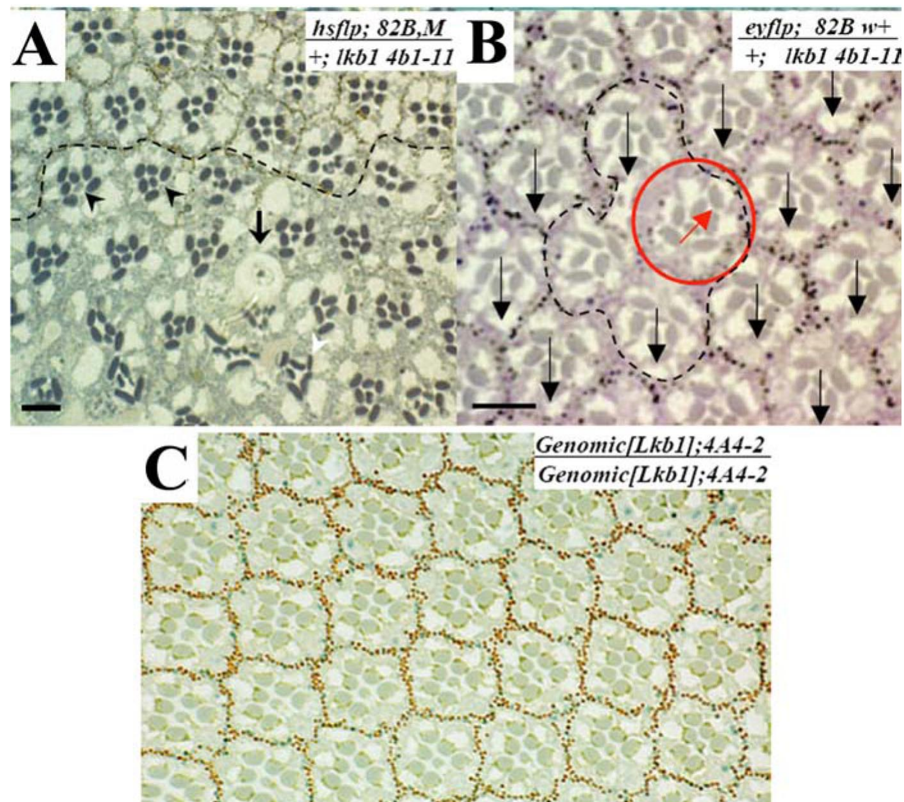

Fig. S1. *lkb1* loss of function in the eye disrupts development, that is rescued by expression of an LKB1 transgene. *lkb1*$^{4B1-11}$ leads to a loss of photoreceptors (black arrowhead), misshapen rhabdomeres (white arrowhead), enlarged cell bodies (black arrow, *A*), and planar polarity defects (red arrow, *B*). (*B*) Planar polarity defect in an *eyflp lkb1*$^{4B1-11}$ clone. In this image, dorsal is up, ventral is down. The circled mutant ommatidia exhibits a dorsal–ventral flip. (*C*) *lkb1*$^{4A4-2}$ defects are rescued by the expression of full length LKB1 under its genomic promoter. (Scale bars, 10 μm.)

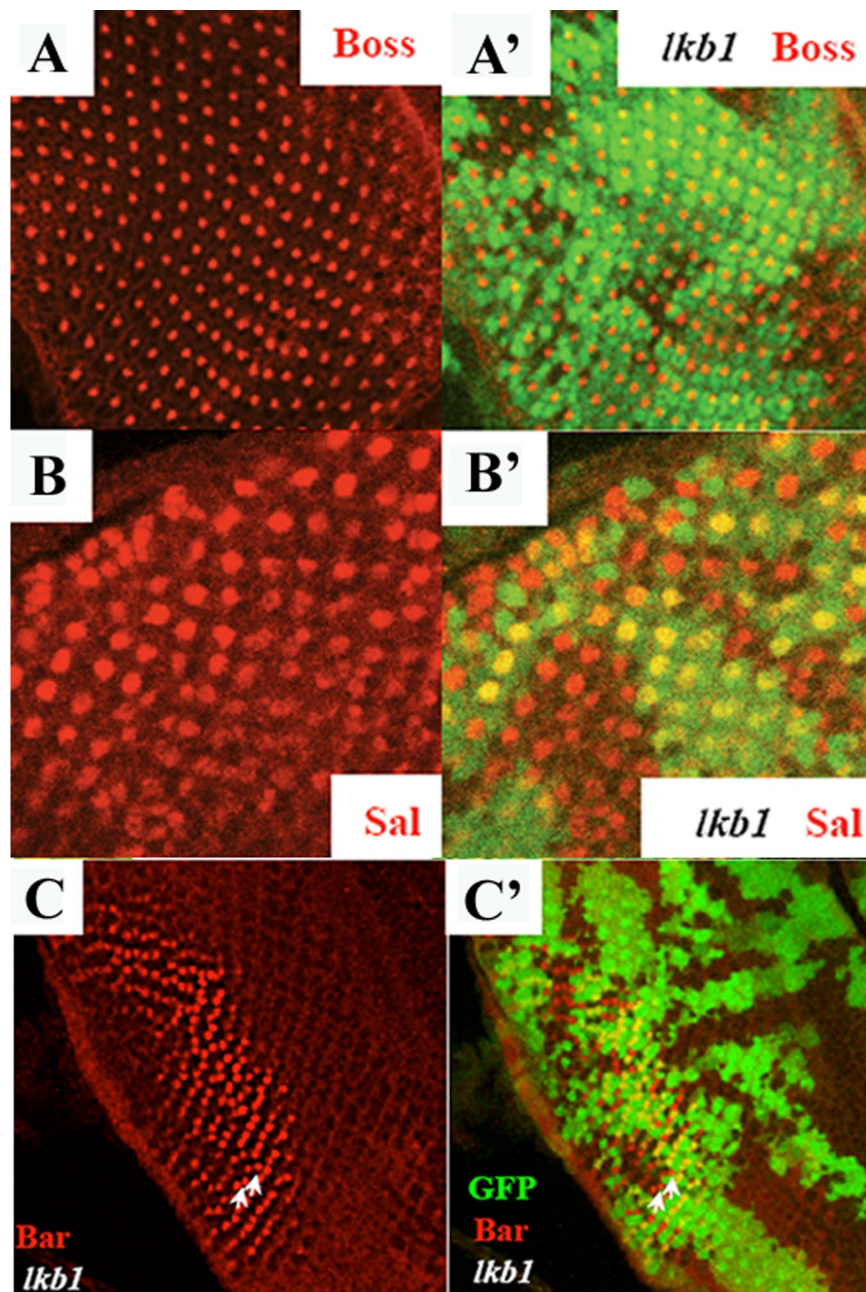

Fig. S2. At the larval stage, lkb1 does not affect photoreceptor differentiation. GFP marks wild-type tissue in all images (green *A–D*, blue *E*. All images shown are *lkb1*^{4A42}. Neuronal markers for individual photoreceptor cells (PRCs) in the third-instar imaginal eye disc show that PRCs 1–8 are correctly specified and positioned in *lkb1*$^{4A4\text{-}2}$ clones. R8 marked by Boss (red) (A and *A*′), R3 and R4 marked by Spalt (red) (*B* and *B*′), and PR 1 and 6 marked by Bar (red) (*C* and *C*′) shows that PRCs in *lkb1* mutant clones are correctly determined and specified. *lkb1* larval clones show mild planar cell polarity defects. Bar (red) marks PR1 and 6, and in wild-type larval eye discs, forms an arrow-like pattern. (*C* and *C*′) *lkb1* clones show occasional planar cell polarity (PCP) defects (white arrowheads).

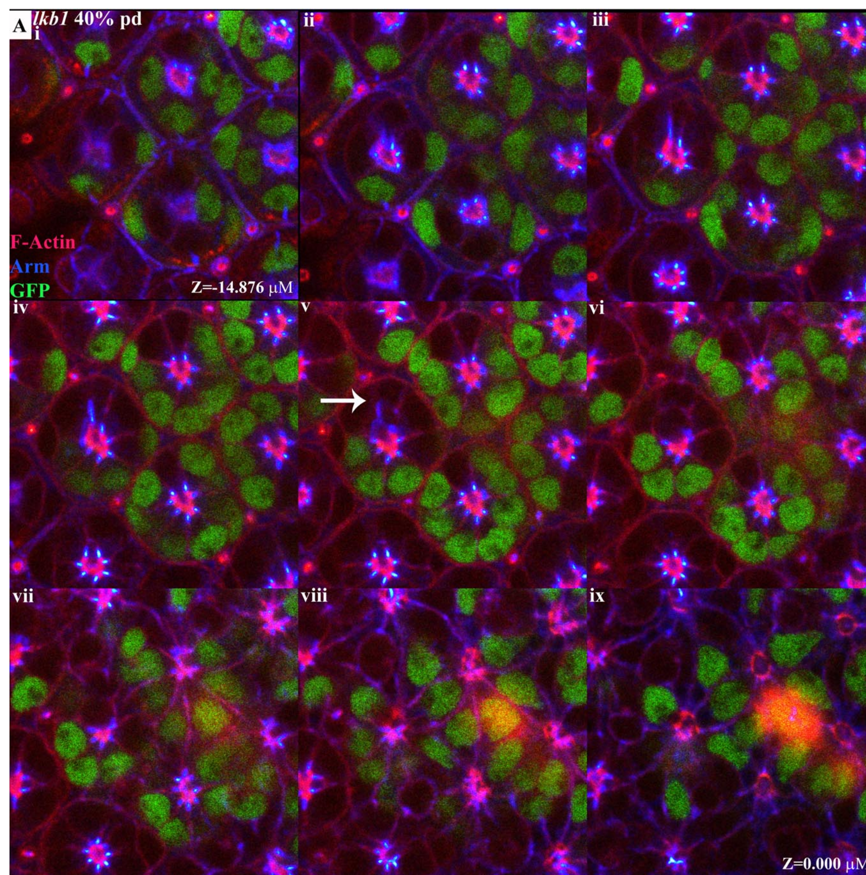

Fig. S3. *lkb1* mutant PRCs extend normally throughout photoreceptor development. Z-sections although a 40% pd *lkb1* mosaic eye, showing wild-type ommatidial cells (green) alongside mutant ommatidal cells. Sections toward the feet show that *lkb1* mutant PRCs fully extend to the same extent as wild type, despite showing defects in Arm localization (arrow). (Scale bars, 5 μm.)

Fig. S4. *lkb1* loss of function results in a disruption of epithelial polarity in the pupal retina. GFP (green) marks wild-type tissue in *B–F* and MARCM clones in *A* and *G*. *lkb1* mutant clones show accumulation of F-actin (red) along the lateral membrane (arrow, *A*). *lkb1*^{4A42} clones also show defects in the localization of apical and junctional markers (*B–E*). The apical marker Crb (red) (arrowheads, *B*) shows expansion into the basolateral domain. Junctional markers Sdt (red) (arrowhead, *C*), DPatJ (green) (arrowhead, *D*), E-Cad (red) (*E*), Arm (blue) (*E′*), Merge of *E* and *E′* (green) (*E′*), and Baz (red) (*F*) also show aberrant expansion into the basolateral domain. (*F*) Baz mislocalization in *lkb1* PRCs (*F1*) Baz mislocalizes apical to Arm (green) (*F2*) *lkb1* ommatidia appear to be fused, and Baz expression appears to be expanded (*F3*) Baz appears to be decreased in levels, despite significant up-regulation of Arm at the junctions. (*F4*) Baz shows an up-regulation in expression, as well as delocalization from Arm expression. (*G*) GFP (green) marks *lkb1* mutant clones expressing P35. Expression of P35 in *lkb1* mutant clones does not rescue *lkb1* (arrow).

Fig. S5. Reduction in the levels of KP78b, NUAK, and SIK homologues phenocopies *lkb1*. (*A*) Wild-type (*yw*) ommatidia show discrete localization of Arm (blue) at the adherens junction, and accumulation of F-actin (red) is shown apical to the adherens junction. (*B*) An example of a severe *lkb1*^{4A42} clone. Arm (blue) and F-actin (red) localization is severely disrupted. (*C–E*) Clones overexpressing AMPK-like RNAi lines are marked with GFP (green). KP78b (*C*), NUAK (*D*), and SIK (*E*) lines, show expansion of Arm (red) toward the basolateral membrane. (Scale bars, 5 μm.)

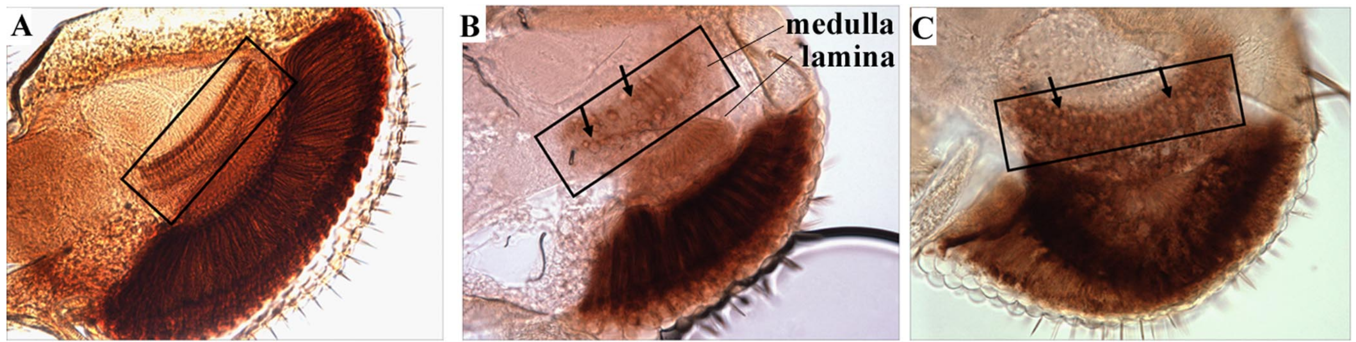

Fig. S6. Both similarities and differences are evident within *lkb1* and *ampk*α mutant adult eyes. Anti-Chaoptin immunohistochemistry (mAb24B10) reveals the photoreceptor axon tracts projecting into the lamina and medulla. The normal termination of axons (*A*) is largely intact in *ampk*α (*B*) and *lkb1* (*C*) mutant axons, however, they both display axonal swellings in the lamina and medulla. (*C*) The lamina and medulla appear fused in *lkb1* mutant retaines, compared to wild type (*A*) and ampkα mutants (*B*).